International Journal of Engineering Research and Development
e-ISSN: 2278-067X, **p**-ISSN: 2278-800X, www.ijerd.com
Volume 7, Issue 3 (May 2013), PP. 33-43

Numerical Simulation of a Batch Fluidized Bed Dryer

I.O Oluwaleye[1], M.B. Adeyemi, S.B. Adeyemo
Department of Mechanical Engineering
Ekiti State University,
P.M.B 5363, Ado Ekiti, Nigeria

Abstract:- The numerical simulation of drying cassava particulates in a batched fluidized bed dryer was undertaken. The dryer consists of a vertical column 400mm diameter with a physical height of 2960mm. A regulated centrifugal blower that generated air flow at three different flow rates (.043 kg/s, 0.05 kg/s and 0.056 kg/s) to fluidize a bed of cassava particulates in turn was powered by a 1.5 Hp electric motor. The air flow was heated by a regulated electric heater to predetermined drying temperature of 120^{o}C. The mass of cassava particulate fed into the dryer per batch is 1.555kg. One dimensional mathematical model based on the two-phase model of Kunni and Levenspiel was used to model the drying process. The data generated were analysed and compared with fluidized and oven drying methods. The result compares well within the limit of the assumptions made for the numerical simulation.

Keywords:- Numerical, Simulation, Drying, Fluidized, Cassava, Particulates

I. INTRODUCTION

Fluidization is the phenomenon of the solid-fluid contacting process in which a bed of solid particles is lifted and agitated by a rising stream of process fluid, thereby making the bed of solid particles behave like fluid [1]. The drying application of fluidization technique to a wide variety of particulate materials in industry dated as far back as 1940s according to Reay [2]. Currently, it is becoming popular for drying crushed minerals, sand, polymers, fertilizers, pharmaceuticals, crystalline materials and many other industrial and agricultural products.

Fluidized drying among others has the advantage of high intensity of drying and high thermal efficiency with uniform and closely controllable temperature in the bed promoted by intensive solid mixing due to the presence of bubbles. It requires less drying time due to high rates of heat and mass transfer. The efficient gas-solid contact leads to compact unit and relatively low capital cost. Since there is no moving parts other than feeding and discharge mechanisms, except in the case of vibrating fluid bed, reliability is high and maintenance cost is low.

A lot of experimental work has been done on the application of fluidized bed for various utilities including drying. Some researchers have worked on different models for simulating drying process for different materials Romamkov [3] according to Hoebink and Rietema[4], Alebregtse[5] Hoebink and Rietema [4] , Verkooijen [6], Passos [7] Theologos, K. N.; Maroulis, Z. B. and Markatos, N.C.[8] , Van Ballegooijen, W.G.E.; Van Loon, A.M. and Van der Zanden, A.J.J. [9]. Wang and Chen [10]] Stakic' and Milojevic' [11]developed a mathematical model to describe the process of unsteady simultaneous heat and mass transfer between gas phase and fine particles during drying process in a fluidized beds of fine particles. They employed a control volume numerical method for the discretization of the differential equations. Their result compared well with experimental existing experimental data.

The model used by [11] was adopted for the simulation of drying process of cassava particulate in a fluidized bed. Preliminary experiments for the determination of the physical and thermal properties of cassava particles for purpose of designing an appropriate dryer and for the simulation of the drying processes were carried out [12]. These properties are: average particle size, density, specific heat capacity, thermal conductivity, porosity and diffusion coefficient. These properties changes as the moisture content decreases with drying.

II. MATHEMATICAL FORMULATION

The mathematical model adopted is based on the work of due Stakic' and Milojevic'[11] which is a two-phase model of Kunni and Levenspiel [1]. The non-dimensional mathematical equations for the model are:

Continuity Equation

$$\frac{\partial \rho_g^*}{\partial t^*} + \frac{\partial (\rho_g^* U_g^*)}{\partial z^*} = S^* \quad \text{---(1)}$$

Energy Conservation Equations

a) Bubble phase

$$\frac{\partial\theta_b}{\partial t^*} + U_b^* \frac{\partial\theta_b}{\partial Z^*} = St_b\, Pe_b\, A_b^* (\theta_g - \theta_b) \qquad \text{(2)}$$

b) **Interstitial gas phase**

$$\frac{\partial\theta_g}{\partial t^*} + U_g^* \frac{\partial\theta_g}{\partial Z^*} = V_b^* St_{bg} Pe_g A_b^*(\theta_b - \theta_g) + V_p^* St_p Pe_g A_p^* (\theta_p - \theta_g) + V_w^* St_{wg} Pe_g A_w^* (\theta_w - \theta_g) + S^*(\theta_g - C^*\theta_p) + S^*T_2^* (1 - C^*) \qquad \text{(3)}$$

c) **Particle phase**

$$\frac{\partial\theta_p}{\partial t} + U_p^* \frac{\partial\theta_p}{\partial z} = \frac{1}{V_p^*} St_p Pe_p A_p^*(\theta_g - \theta_p) + \frac{V_w^*}{V_p^*} St_w Pe_p A_w^* (\theta_w - \theta_p) + \frac{r^* S^* \rho_1^*}{V_p^*} + \frac{\partial^2\theta_p}{\partial Z^{*2}} \qquad \text{(4)}$$

Humidity Content Conservation Equations

a) **Bubble phase**

$$\frac{\partial G_{vb}}{\partial t^*} + U_b^* \frac{\partial G_{vb}}{\partial Z^*} = \frac{Sh_b}{Le} A_b^*(G_{vg} - G_{vb}) \qquad \text{(5)}$$

b) **Interstitial gas phase**

$$\frac{\partial G_{vg}}{\partial t^*} + U_g^* \frac{\partial G_{vg}}{\partial Z^*} = \rho_2^* V_b^* \frac{Sh_b}{Le} A_b^*(G_{vb} - G_{vg}) + V_p^* \frac{Sh_p}{Le} A_p^* (G_{vs} - G_{vg}) + S^*\rho_3^* (G_{vg} - G_{vs}) \qquad \text{(6)}$$

c) **Particle phase**

$$\frac{\partial W_p}{\partial t^*} + U_p^* \frac{\partial W_p}{\partial Z^*} = \rho_4^* \frac{Sh_p}{Le} A_p^*(G_{vg} - G_{vs}) + \frac{1}{Le} \frac{\partial^2 W_p}{\partial Z^{*2}} \qquad \text{(7)}$$

The normalizing parameters are defined as:

$$t^* = \frac{\alpha t}{H_B^2} \; ; \; \rho^* = \frac{\rho R T_1}{P_1} \; ; \; Z^* = \frac{Z}{H_B} \; ; \; U^* = \frac{H_B U}{\alpha} \; ; \; \theta = \frac{T - T_2}{T_1 - T_2}$$

$$S^* = \frac{\rho_m^*}{t^*} = \frac{\rho_m R T_1 H_B^2}{t P_1 \alpha} = \frac{S_m^p R T_1 H_B}{P_1 U_{mf}} \qquad \text{(8)}$$

Explicit finite difference scheme and stability criterion

An explicit finite difference scheme was used to simplify the partial differential equations (1) – (7), and to ensure stability of the scheme, RitchMeyer stability criterion was adopted. The resulting finite difference equations are as follows:

$$S^* = \frac{\rho_{a,j}^{n+1} - \rho_{a,j}^{n}}{\Delta t^*} = \frac{\Delta\rho_a}{\Delta t} \qquad \text{(9)}$$

$$\theta_{b,j}^{n+1} = \left(1 - \frac{\Delta t_b^*}{\Delta z^*} U_{b,j}^* - St_b\, Pe_b\, A_b^*\, \Delta t_b^*\right)\theta_{b,j}^{n} + \frac{\Delta t_b^*}{\Delta z^*} U_{b,j}^*\, \theta_{b,j-1}^{n} + St_b\, Pe_b\, A_b^*\, \Delta t_b^*\, \theta_{g,j}^{n} \quad \text{-------(10)}$$

$$\theta_{g,j}^{n+1} = \theta_{g,j}^{n}\left(1 - \frac{\Delta t_g^*}{\Delta z^*} U_{g,j}^* - V_b^*\, St_{bg}\, Pe_g\, A_b^*\, \Delta t_g^* - V_p^*\, St_p\, Pe_g\, A_p^*\, \Delta t_g^* - V_w^*\, St_{wg}\, Pe_g\, A_w^*\, \Delta t_g^* + \Delta t_g^* S^*\right)$$
$$+ \frac{\Delta t_g^*}{\Delta z^*} U_{g,j}^*\, \theta_{g,j-1}^{n} + V_b^*\, St_{bg}\, Pe_g\, A_b^*\, \Delta t_g^*\, \theta_{b,j}^{n} + \left(V_p^*\, St_p\, Pe_g\, A_p^*\, \Delta t_g^* - S^*\, \Delta t_g^*\, C^*\right)\theta_{p,j}^{n} +$$
$$V_w^*\, St_{wg}\, Pe_g\, A_w^*\, \Delta t_g^*\, \theta_{w,j}^{n} + S^* \Delta t_g^*\, T_2^*\, (1 - C^*) \quad \text{------(11)}$$

$$\theta_{p,j}^{n+1} = \theta_{p,j}^{n}\left(1 - \frac{\Delta t_p^*}{\Delta z^*} U_{p,j}^* - \frac{\Delta t_p^*}{V_{p,j}^*} St_p\, Pe_P\, A_p^* - \frac{V_{w,j}^*}{V_{p,j}^*} St_w\, \Delta t_p^*\, A_w^*\, Pe_P - \frac{2\Delta t_p^*}{\Delta z^{*2}}\right) +$$
$$\frac{\Delta t_p^*}{V_{p,j}^*} St_p\, Pe_p\, A_p^*\, \theta_{g,j}^{n} + \frac{V_{w,j}^*}{V_{p,j}^*} St_w Pe_p\, A_w^*\, \Delta t_p^*\, \theta_{w,j}^{n} + \frac{\Delta t_p^*}{\Delta z^{*2}} \theta_{p,j+1}^{n} + \left(\frac{\Delta t_p^*}{\Delta z^{*2}} + \frac{\Delta t_p^*\, U_{p,j}^*}{\Delta z^*}\right)\theta_{p,j-1}^{n} +$$
$$\frac{r^*\, S^* \rho_1^*}{V_p^* \rho_{pd}^*} \quad \text{------(12)}$$

$$G_{vb,j}^{n+1} = \left(1 - \frac{\Delta t_{vb}^*}{\Delta z^*} U_{b,j}^* - \frac{Sh_b}{Le} A_b^* \Delta t_{vb}^*\right) G_{vb,j}^{n} + \frac{\Delta t_{vb}^*}{\Delta z^*} U_{b,j}^*\, G_{vb,j-1}^{n} + \frac{Sh_b}{Le} \Delta t_{vb}^*\, A_b^*\, G_{g,j}^{n} \quad \text{------(13)}$$

$$G_{vg,j}^{n+1} = G_{vg,j}^{n}\left(1 - \frac{\Delta t_{vg}^*}{\Delta z^*} U_{g,j}^* - \rho_2^* V_b^* \frac{Sh_b}{Le} A_b^* \Delta t_{vg}^* - V_p^* \frac{Sh_p}{Le} A_p^* \Delta t_{vg}^* + S^* \rho_3^* \Delta t_{vg}^*\right) +$$
$$\frac{\Delta t_{vg}^* U_{g,j}^*}{\Delta z^*} G_{vg,j-1}^{n} + \rho_2^* V_b^* \frac{Sh_b}{Le} A_b^* \Delta t_{vg}^* G_{vb,j}^{n} + \left(V_p^* \frac{Sh_b}{Le} A_p^* \Delta t_{vg}^* - S^* \rho_3^* \Delta t_{vg}^*\right) G_{vs,j}^{n} \quad \text{---(14)}$$

$$W_{P,j}^{n+1} = W_{p,j}^{n}\left(1 - \frac{\Delta t_{wp}^*}{\Delta z^*} U_{p,j}^* - \frac{2\Delta t_{wp}^*}{Le\, \Delta z^{*2}}\right) + \left(\frac{\Delta t_{wp}^*}{\Delta z^*} U_{p,j}^* + \frac{\Delta t_{wp}^*}{Le\, \Delta z^{*2}}\right) W_{p,j-1}^{n} +$$
$$\frac{\Delta t_{wp}^*}{Le\, \Delta z^{*2}} W_{p,j+1}^{n} + \rho_4^* \frac{Sh_p}{Le} A_p^* \Delta t_{wp}^* G_{vg,j}^{n} + \rho_4^* \frac{Sh_p}{Le} A_p^* G_{vs,j}^{n} \Delta t_{wp}^* \quad \text{------(15)}$$

Numerical computational grid

The dryer column and numerical computational grid is shown in Fig 1. There is symmetry about the center line CC

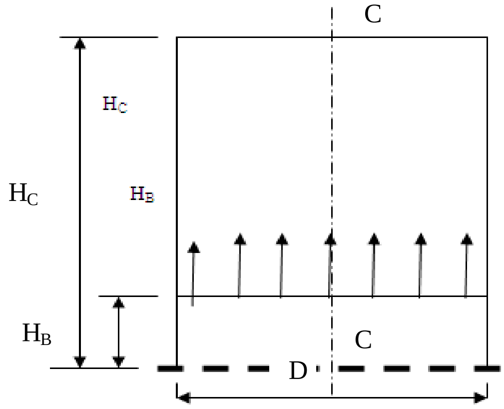

Fig 1: Numerical computational grid

Initial Conditions
t = 0 i.e before feeding the column with cassava particulate sample to be dried.

$\theta_{b,j} = \theta_{g,j} = 1$ --(1)

$\theta_{p,j} = 0$ ---(2)

Gvb = Gvg = Gvs = G = 0.000129T -0.00067----------(3)

$W_p = 100\%$ -----------------------------(4)

$$H_B = \frac{4m_g}{\rho_P \pi Di^2} \text{ ------(5)}$$

Mass flow rate = $0.002118\rho \sqrt{[(2\rho_k g\Delta H)/\rho]}$ kg/s

Density of manometric liquid used, $\rho_k = 804$ kg/m^3 g = 9.81m/s^2

From standard table of properties of air, $\rho = 1.27\text{-}3.29E\text{-}03T + 3.84E\text{-}06T^2$

Mass flow rate = $0.002118 \sqrt{(2\rho_k g\Delta H)} \sqrt{(1.27\text{-}3.29E\text{-}03T+3.84E\text{-}06T^2)}$ kg/s ---------------(6)

Thermal diffusivity, $\alpha = 0.147538 + 0.001829T$

$$U_g^* = \frac{4m_g \{0.01684\sqrt{(2\rho_k g\Delta H)} \sqrt{(1.27\text{-}3.29E\text{-}03T+3.84E\text{-}06T^2)}\}}{\alpha\rho_P\pi Di^2(1.27\text{-}3.29E\text{-}03T+3.84E\text{-}06T^2)} \text{ ------(7)}$$

$U_b^* = 0$ ---(8)

$U_p^* = 0$ ---(9)

$S^* = 0$ ---(10)

Boundary conditions

At the distributor grid, i.e at Z = 0 at all t before the critical time t_c .

$\theta_{b,0} = \theta_{g,0} = 1$ ---(11)

$$U_{g,0}^* = \frac{4m_g \{107.841\sqrt{(2\rho_k g\Delta H)} \sqrt{(1.27\text{-}3.29E\text{-}03T+3.84E\text{-}06T^2)}\}}{\alpha\rho_P\pi Di^2(1.27\text{-}3.29E\text{-}03T+3.84E\text{-}06T^2)} \text{ ------(13)}$$

$$U_{b,0}^* = \frac{H_B U_b}{\alpha} \text{ ------(14)}$$

$U_{p,0}^* = 0$ (No slip factor)--(15)

The absolute humidity ratio, Gvb = Gvg = Gvs = G = 0.000129T -0.00067

Boundary conditions : At the exit of the column i.e Z =1

$$U_g^* = \frac{4m_g\{0.01684\sqrt{(2\rho_k g\Delta H)}\sqrt{(1.27-3.29E-03T+3.84E-06T^2)}\}}{\alpha\rho_P\pi Di^2(1.27-3.29E-03T+3.84E-06T^2)} \quad (23)$$

U_b^* = 0 (Bubble has already collapse at the surface of bed height, at exit no bubble) ---(24)

U_p^* = 0 (No particle exit the column) ---(25)

III. RESULTS AND DISCUSSION

The governing equations of fluidizing drying operations in simplified forms are parabolic differential equations (see equations (1-8). The governing equations of the problems are boundary bound and matching in time. The finite difference expressions of the governing equations are given in equations (9-16) in chapter two. To ensure the stability of the scheme, RitchMeye stability criterion was employed. The least time interval was used for the simulation. The constants parameters in these expressions are properties of cassava particles and are functions of the moisture contents. The experimental correlations were determined by [12] and were used for the numerical simulations.

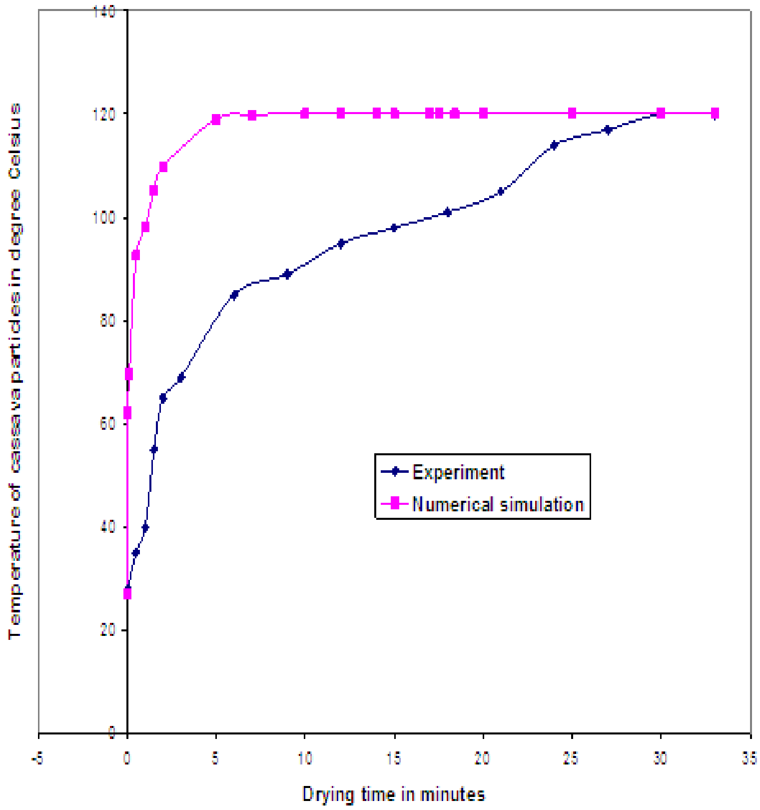

Fig 2: Typical numerical and experimental temperature of cassava particles versus drying time at 0.043kg/s and at 120°C drying temperature

Fig 2 shows the air particle temperature versus drying time at 120°C drying temperature for both experimental and numerical simulation at an air flow rate of **at 0.043kg/s**. As soon as the wet particles got in contact with the stream of hot air the temperature of cassava particles begin to rise while that of the hot air fell initially and then gradually increased.

In Fig 3, the moisture ratio versus drying time for numerical simulation at 120°C drying temperature for various air flow rates of 0.043kg/s, 0.05kg/s and 0.056kg/s are as shown. The diffusion model constants for Fig 2 obtained from regression analysis is shown in Table 1. From the Fig 3, after about 1 hr of drying, the the moisture ratio of particles at a lesser air flow rate is less than at higher air flow rate. The resident time of streams of hot air within the bed affect the rate of drying being the only source of heat available for drying. When compared with the result of oven and fluidized dryers, the result is shown in Fig 4 and Table 2

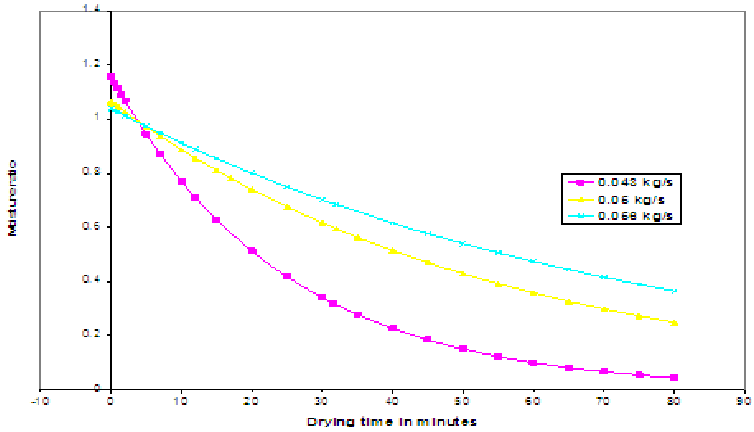

Figure 3: Moisture ratio versus drying time for numerical simulation at 120°C drying temperature for various air flow rate

Table 1: Diffusion Model Constants for numerical simulation at isothermal temperature for various air flow rate obtained from regression analysis

Diffusion Constants	Drying Temperature 120°C		
	0.043 kg/s	0.05 kg/s	0.056 kg/s
K_0	-0.04082	-0.01815	-0.01308
B_0	1.159037	1.064158	1.039555
Coefficient of correlation r	-0.81916	-0.90208	-0.93541

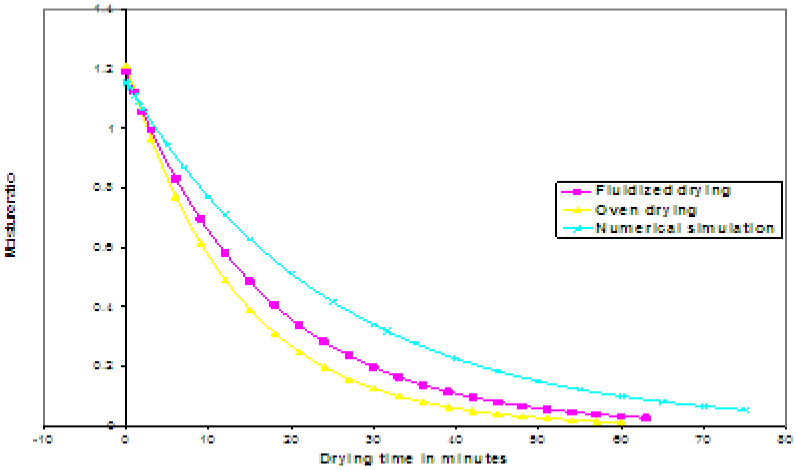

Fig. 4: Comparative Moisture ratio versus drying time of cassava particles using oven drying, fluidized bed drying and numerical simulation at 120°C and at air flow rate of 0.043 kg/s

Table 2 : Diffusion Model Constants at isothermal drying temperature 120°C using oven drying, fluidized bed methods and numerical simulation at air flow rate of 0.043 kg/s obtained from regression analysis

Diffusion Constants	Drying Temperature 120°C		
	Oven	Fluidized bed	Numerical
K_0	-0.07545	-0.0582	-0.04082
B_0	1.2139	1.17693	1.159037
Coefficient of correlation r	-0.99018	-0.97351	-0.81916

The drying rate versus free moisture content at 120°C degree drying rate at various air flow rates are shown in Fig 5. The lower air flow rate gave us a higher drying rate as indicated in the Figure. A table of critical free moisture content and drying rate for numerical simulation at various air flow rate and at 120°C temperatures is shown in Table 3

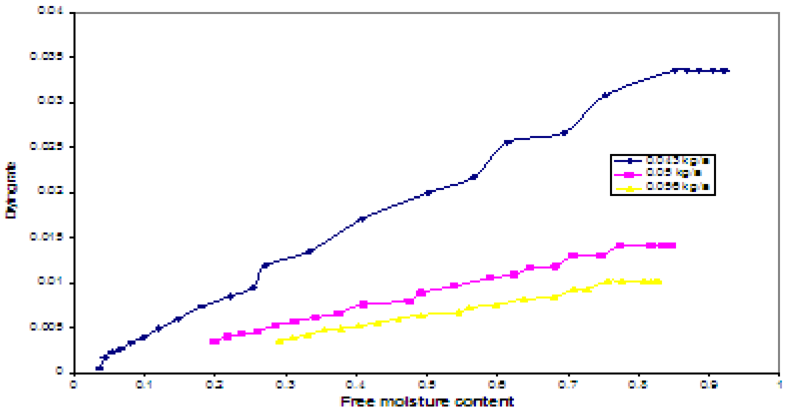

Fig 5: Drying rate versus free moisture content at various air flow rate and at 120 °C drying temperature

Table 3: Critical free moisture content and drying rate for numerical simulation at various air flow rate and at 120°C temperatures

	Air flow rates		
	0.043kg/s	0.05kg/s	0.056kg/s
Critical free moisture Xc	0.752548	0.706738	0.707551
Critical drying rate Rc	0.0308	0.00131	0.00938
Constant drying rate	0.0336	0.0142	0.01027

A comparative rate of drying for oven drying, fluidized bed drying [13] and numerical simulation is shown in Fig 6 and a table of critical free moisture in Table 4

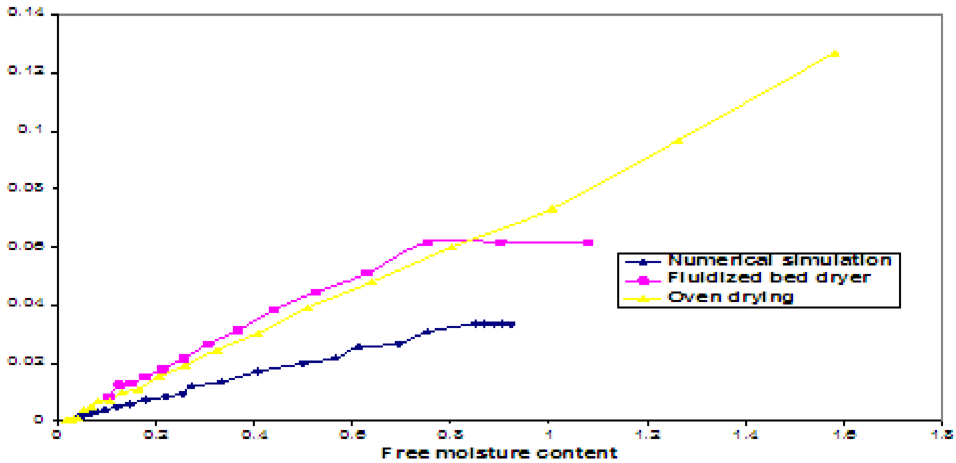

Figure 6: Comparative drying rates versus free moisture content of oven drying, fluidized drying methods and the numerical simulation.

Table 4: Critical free moisture content and drying rate for oven drying, fluidized bed dryer and numerical simulation at the same drying temperature and at air flow rate of 0.043 kg/s

	At 120°C		
	Oven	Fluidized bed	Numerical
Critical free moisture Xc	1.2612	0.6296	0.7526
Critical drying rate Rc	0.0967	0.0509	0.0308
Constant drying rate	0.127	0.0618	0.0336

IV. CONCLUSION

The numerical model for the drying of cassava particle approximate the drying process within the limit of the approximations for the governing equations. The flow process of one dimension was assumed for the numerical simulation but the temperature distribution of air at 23 cm above the distributor of the fluidized bed dryer is symmetry about the radius. It shows that two dimensional governing equations will give a better approximate solution to drying process within the dryer column of diameter 0.4 m and above.

Acknowledgement
The authors are grateful to the Ekiti State University, Ado Ekiti, Nigeria for the financial support for this research.

NOMENCLATURE

A Specific surface m^{-1}
A_o Catchment area m^{-2}
Ar Archimedes number
A_C Duct area of cyclone
C_{pg} Gas specific heat capacity J/Kgk
C_{pp} Particle specific heat capacity J/KgK
C_{pv} Vapour specific heat capacity J/KgK
C_d Coefficient of discharge
d Diameter m
D_{BC}, D_i Fluidized-bed column diameter
d_{eq} Equivalent bubble diameter
d_p Particle(mean sieve) diameter
d_{or} Diameter of distributor orifice

Da Darcy number = $\frac{\mathbf{K}}{H^2}$

D_e Effective diffusion coefficient m^2/s
F_{or} Fractional open area of distributor
g Acceleration due to gravity m/s^2
G Gas humidity i.e ratio of mass of water vapour in a given volume of mixture to the mass of air in the same volume

Gr Grashof number = $\frac{g \beta \Delta T H^3}{\nu^2}$

H_B Bed Height m
H_C Height of the physical column
h Heat transfer coefficient W/m^2K
h_m Mass transfer coefficient m/s
K Permeability (m^2)
k Effective thermal conductivity W/m^2K
K_n Resistance for moisture movement within the material

Le Lewis number = $\frac{Sc}{Pr} = \frac{\alpha}{D}$

m Mass flow rate Kg/s
M_{mf} Mass flow rate at minimum fluidization
N= Number of orifice
m_g Mass of saturated vapour
m_v Mass of water vapour
m_a Mass of dry air (without vapour)
M Molecular mass Kg/mol
N Number of orifice

h H

NU Nusselt number = $\frac{\quad}{k}$

P Atmospheric Pressure Pa

P_a Pressure of air

P_v Pressure of vapour

P_g Saturated vapour pressure

Pr Prandtl number = $\frac{\nu}{\alpha}$

Pe Peclet number = $\frac{U_\infty H}{\alpha}$

r Energy of water phase exchange, Radius J/Kg, m

Ra Rayleigh number = $\frac{g\,\beta\Delta T H^3}{\nu\,\alpha}$

Ra_m Darcy-modified Rayleigh number = $\frac{\mathbf{K} g\,\beta\Delta T H}{\nu\,\alpha}$

Re Reynolds number = $\frac{\rho U\,H}{\mu}$

R_a Gas constant for air = 0.289kJ/kgK

R_v Gas constant for water vapour = 0.4615kJ/kgK

S_m^P Rate of mass generation per unit volume during drying (density of moisture /time)

Sc Schmidts number = $\frac{\nu}{D}$

S centre to centre hole spacing

Sh Sherwoods number = $\frac{h_m H}{D}$

St Stanton number = $\frac{h}{\rho C_p U_\infty} = \frac{hH}{\rho C_p\,\alpha} = \frac{h_m}{U_\infty} = \frac{h_m H}{\alpha} = \frac{NU}{Pr\,Re}$

St_V Stanton number for mass transfer = $\frac{Sh}{Re\,Sc}$

t Time (second, s)

T Temperature (Kelvin, K)

U Velocity (m/s)

V_{BC} Volume of settled bed

U_{mf} Minimum fluidization velocity

V Volume (m^3)

W Moisture content of solid = $(W_{wet} - W_{dry})/W_{dry}$ (kg/kg) (on dry basis)

W Moisture content of solid = $(W_{wet} - W_{dry})/W_{wet}$ (kg/kg) (on wet basis)

Wc Drying flux (Rate of moisture removal) (Kg/m^2s)

Z Axial co-ordinate axis (m)

SUBSCRIPTS:

b Bubble
bc Cloud to bubble
be Emulsion to bubble
B Bed
c Constant-rate period
ce Emulsion to cloud
d distibutor
0 initial
1 Entry point to the fluidized bed
2 Outlet point of the fluidized bed
e Effective
g Gas
mf Minimum fluidization
o orifice

pg Particle in gas phase
r room
s Surface
wp wall/particle
pd Particle in dense phase
vg Vapour/gas
vb Vapour/bubble
vs Vapour/surface
w Wall

GREEK LETTERS:

α Alpha (thermal diffusivity)
ν Nu (kinematic viscosity)
ρ Rho (density)
K (Permeability)
μ Mu (dynamic viscosity)
ϕ Relative humidity
θ Nondimensional temperature $= \dfrac{T - T_r}{T_1 - T_r}$
ε Particle voidage

p Particle

REFERENCES

[1]. Daizo Kunii and Octave Levenspiel (1991), Fluidization Engineering, Butterworth-Heinemann, USA, pp 1-13, 15-58

[2]. Reay, D. (1986), Fluid Bed Drying, In Gas Fluidization Technology, Ed. By D.Geldart, John Wiley and Sons, pp. 259-284,

[3]. Romankov, P.G.(1971), Drying, In Fluidization , Ed. By Davidson J. F. and Harrison D., Academic Press, London

[4]. Hoebink, J.H.B.J and Rietema, K. (1980), Drying Granular Solids in Fluidized Bed I and II, Chemical Engineering Science, Vol 35, pp 2135-2140 and pp 2257-2265

[5]. Alergregtse Johan B (1986), Fludized Bed Drying: A Mathematical Model for Hydrodynamics and Mass Transfer, In Heat and Mass Transfer in Fixed And Fluidized Beds by W.P.M Van Swaaij and N.H/ Afgan, Hemisphere Publishing Corporation, PP 511-521

[6]. Verkooijen A.H.M,(1986), Fluidized Bed Drying of Fine Particles with Internal Diffusion Limitation, In Fluidization V: Proceedings of the fifth Engineering Foundation Conference on Fluidization, May 18-23, Elsinore Denmark, Ed. By ∅stergaard, K and S∅rensen, A. Engineering Foundation, New York pp. 643-649

[7]. Franca, A. S.; Passos; M. L., (1997),Finite element analysis of gas flow in spouted be dryers, Proceedings of the ASAE Annual International Meeting. Part 1 oF (3), Universidade Federal de Minas Gerais, Belo Horizonte, Braz, Minneapolis, MN, USA, Conference.

[8]. Theologos, K. N.; Maroulis, Z. B.; Markatos, N.C. (1997), Simulation of transport dynamics in fluidized-bed dryers, Drying Technology v 15 n 5 May., National Technical University of Attens, Greece. pp 1265-1291

[9]. Van Ballegooijen, W.G.E.; Van Loon, A.M. and Van der Zanden, A.J.J. (1997), Modeling diffusion-limited drying behaviour in a batch fluidized bed dryer, Drying Technology v15 n3-4 March – April, Eindhoven University of Technology, Eindhoven, Netherland.pp 837-855

[10]. Wang, Zhao Hui and Chen Guohua(2000), Heat and mass transfer in batch fluidized-bed drying of porous particles, Chemical Engineering Science v55 n10 May 2000, Hong Kong University of Science and Technology, Kowloon, Hong Kong. pp 1857-1869

[11]. Stakic', M..B. and Milojevic', D.Z. (1991), Numerical Simulation of Fluidized Bed Drying Processes, In Drying '91 Ed. By Mujumdar A.S and Filkova', Elsevier Science Publishers, Amsterdam, pp. 251-257

[12] **Ogunleye, I.O**, Adeyemo, S.B. and Adeyemi, M.B. (2007), "Effects of Moisture Content on the Physical, Thermal and Isothermal Drying Properties of Granular Cassava Particles", Journal of Engineering and Applied Sciences 3 (5) pp 416-423, Pakistan

[13] Oluwaleye, I.O. and Adeyemi, M.B.(2013), "Experimental Evaluation of a Batch Hot Air Fluidized Dryer", International Journal of Modern Engineering Research vol 3, Issue 1, Jan-Feb 2013, pp 497-503